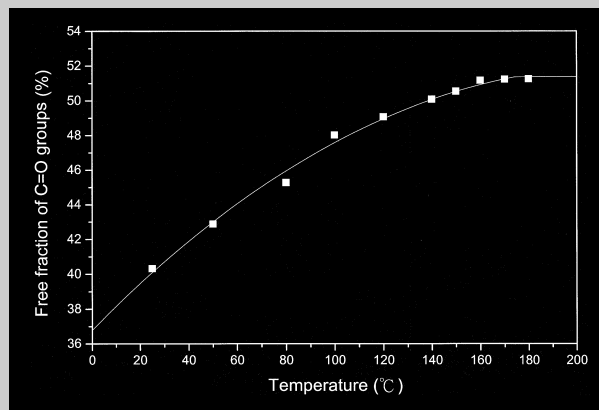**Full Paper:** The miscibility behavior and specific interaction of phenolic resin with poly(acetoxystyrene) (PAS) blends were examined using differential scanning calorimetry (DSC), fourier-transform infrared (FT-IR) spectroscopy and solid-state NMR. This phenolic/PAS blend is fully miscible, as indicated by a single glass-transition temperature, due to the formation of inter-hydrogen bonding between the hydroxyl group of the phenolic resin and the carbonyl group of PAS. The DSC study indicates that this phase-separation exothermic peak area is closely related to the interaction between the components. Furthermore, ^{13}C solid-state NMR and FT-IR spectroscopies were used to study the extent of specific interaction with various compositions and degrees of inter- and intramolecular hydrogen bonding. Moreover, the inter-association equilibrium constant and the related enthalpy of this phenolic/PAS blend were determined and used to predict the free energy and fraction of the hydrogen bonding according to the Painter–Coleman association model.

The fraction of free carbonyl groups versus temperature for the phenolic/PAS = 50:50 blend.

Miscibility Behavior and Specific Interaction of Phenolic Resin with Poly(acetoxystyrene) Blends

Shiao Wei Kuo, Feng Chih Chang*

Institute of Applied Chemistry, National Chiao Tung University, Hsin Chu, Taiwan, Republic of China
Fax: 886-3-5723764; E-mail: changfc@cc.nctu.edu.tw

Introduction

The miscibility of polymer blends has attracted significant attention in polymer science. For nonpolar polymer blends, the miscibility can be roughly estimated using the Flory–Huggins polymer solution theory presented in Equation (1):

$$\frac{\Delta G_N}{RT} = \frac{\Phi_1}{N_1}\ln\Phi_1 + \frac{\Phi_2}{N_2}\ln\Phi_2 + \Phi_1\Phi_2\chi_{12} \qquad (1)$$

where Φ and N denote the volume fraction and the number of segments, respectively, χ represents the so-called Flory–Huggins interaction parameter calculated by Hilderbrand's solubility parameter, and subscripts 1 and 2 refer to the blend compounds. In the case of high-molecular-weight polymers, N_1, $N_2 \gg 1$, and consequently, the first two entropy terms become vanishingly small and the miscibility becomes increasingly dependent on the nature of the contribution of the enthalpic term. To enhance the

formation of a one-phase miscible system in polymer blends, it is necessary to ensure that favorable specific intermolecular interaction exists between the two base components of the blend. Ideally, one polymer possesses donor sites and the other possesses acceptor sites on the chain. The most commonly observed interactions are the general acid–base type, i.e., hydrogen bonding,[1–4] ion-dipole, or charge-transfer interaction.

Painter and Coleman[5] suggested adding an additional term to account for the free energy of the hydrogen bonding formation into the simple Flory–Huggins expression for the free energy of mixing of two polymers, as in Equation (2):

$$\frac{\Delta G_N}{RT} = \frac{\Phi_1}{N_1}\ln\Phi_1 + \frac{\Phi_2}{N_2}\ln\Phi_2 + \Phi_1\Phi_2\chi_{12} + \frac{\Delta G_H}{RT} \qquad (2)$$

Here ΔG_H denotes the free-energy change contributed by the hydrogen bonding between two components,

which can be estimated from FT-IR spectroscopy. This equation neglects the change in free volume and other complications.[6]

Phenolic resin contains a high density of hydroxyl groups that can interact with numerous other polymers through hydrogen bonding. Hydrogen bonding serves as a physical crosslink in phenolic resin and increases the glass-transition temperature (T_g). The Novolac-type phenolic resin possesses a higher T_g than other materials with a similar molecular weight because of the high density of its hydrogen bonds. When phenolic resin is blended with poly(acetoxystyrene) (PAS), the resultant T_g is significantly lower than the value predicted with the Fox rule (see later), indicating that the blend system must involve some special interaction. This work investigates the interaction between phenolic resin and PAS caused by the association of hydroxyl and carbonyl groups.

The carbonyl stretching vibration has been proven to be an excellent indicator of molecular interaction for a number of polymers.[7–13] The repeated PAS unit inhibits the self-association of the phenolic hydroxy groups that causes the T_g of the phenolic/PAS blends to be lower than predicted.

This work employs the association parameter of the Painter–Coleman association model (PCAM) to investigate the thermodynamic properties of the phenolic/PAS blends and predict the free energy and fraction of hydrogen bonding.

Experimental Part

Materials

The phenolic resin was synthesized with sulfuric acid via a condensation reaction producing average molecular weights $\overline{M}_n = 500$ and $\overline{M}_w = 1200$. The chemical structure of the Novolac-type phenolic resin was determined from the solution ^{13}C NMR spectrum, and found to contain 0.15 wt.-% free phenol, consisting of phenol rings bridge-linked randomly by methylene groups with 19% *ortho–ortho*, 57% *ortho–para*, and 24% *para–para* methylene bridges.[14,15] The phenolic resin does not contain any reactive methylol group which is capable of causing crosslinking on heating.

PAS was obtained through radical polymerization of the *p*-acetoxystyrene monomer using 2,2′-azoisobutyronitrile (AIBN) initiator (1 wt.-% based on the monomer) at 60 °C under a nitrogen atmosphere. The product was dissolved in benzene, and the solution was poured into the vigorously stirred methanol to precipitate the polymer. The polymer was then characterized using FT-IR spectroscopy, differential scanning calorimetry (DSC), and gel permeation chromatography (GPC). The synthesized PAS is characterized by T_g at 122 °C, $\overline{M}_n = 21\,500$ and $\overline{M}_w$ 35 000. The chemical structures of phenolic resin and PAS and their atom-numbering schemes are illustrated in Figure 1.
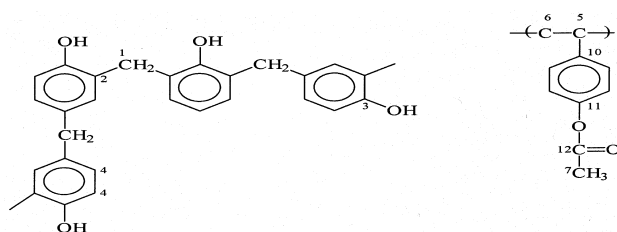

Figure 1.   Chemical structures of the phenolic polymer (left) and PAS (right) and their atom-numbering schemes.

Blend Preparation

Blends of phenolic/PAS with various compositions were prepared by solution blending. Tetrahydrofuran solution containing 5 wt.-% polymer mixture was stirred for 6–8 h, and the solution was allowed to evaporate slowly at room temperature for 1 d. The film of the blend was then dried at 50 °C for 2 d.

Characterizations

DSC

T_gs of blend films were determined by using a DSC from Du-Pont (DSC-9000) at scan rate of 20 °C · min^{-1} and a temperature range of 30–125 °C. The measurement was taken using a 5–10-mg sample on a DSC sample cell after the sample was quickly cooled to −50 °C from the melt of the first scan. The T_g occurs at the midpoint of the heat capacity transition between the upper and lower points of deviation from the extrapolated liquid and glass lines.

FT-IR Spectroscopy

FT-IR spectra were measured using a Nicolet Avatar 320 FT-IR spectrophotometer and 32 scans were collected with a spectral resolution of 1 cm^{-1}. Samples containing hydroxyl groups are water sensitive, so a pure nitrogen flow was used to purge the IR optical box to prevent the sample film from being exposed to moisture. IR spectra recorded at elevated temperatures were obtained using a cell mounted inside the temperature-controlled compartment of the spectrometer. For the solution sample, an adequately sealed cell with NaCl windows and 0.05-mm sample thickness was used. A single optical path was used to study the inter-association equilibrium constant between model compounds of 2,4-dimethylphenol and *p*-tolyl acetate. All model compound solutions in the absorption range obey the Beer–Lambert law. Cyclohexane was selected as the solvent because the specific conformation of the cyclohexane is favorable in this study.

Solid-State NMR Spectroscopy

High-resolution solid-state ^{13}C NMR experiments were carried out on a Bruker DSX-400 Spectrometer operating at resonance frequencies of 399.53 and 100.47 MHz for ^{1}H and ^{13}C, respectively. The ^{13}C CP/magic-angle sample spinning (MAS) spectra were measured with a 3.9-μs 90° pulse, a 3-s pulse delay time, an acquisition time of 30 ms and 2048

scans. All NMR spectra were taken at 300 K using broad-band proton decoupling and a normal cross-polarization pulse sequence and a MAS rate of 5.4 kHz was used to avoid absorption overlapping.

Results and Discussion

Thermal Analyses

In a polymer blend, a single, composition-dependent glass transition indicates full miscibility with a dimension in the order of 20–40 nm. Single T_g behavior represents macroscopic evidence of the full miscibility of the blend. The DSC analyses of Figure 2 reveal the monotonic T_g behavior from all compositions as would be expected for a miscible blend; T_gs of pure phenolic resin and pure PAS occur at 66.3 °C and 122.3 °C, respectively. Various equations have been designed to predict the variation of the T_g of a random copolymer or miscible blend as a function of composition. The most widely used equation is the Kwei equation:[16]

$$T_g = \frac{W_1 T_{g1} + kW_2 T_{g2}}{W_1 + kW_2} + qW_1 W_2 \qquad (3)$$

where W_1 and W_2 denote weight fractions of the compositions, T_{g1} and T_{g2} represent the T_gs of the corresponding blend components, and k and q are fitting constants. The Kwei equation can be applied to miscible polymer blends with a specific interaction. Figure 3 shows plots of the T_g of the blend versus its composition for cases where the Gordon–Taylor[17] and Fox equation[18] do not fit well from the experimental data. However, the Kwei equation can correlate well with the experimental data. Based on the non-linear least squares "best fit", $k = 1$ and $q = -245$
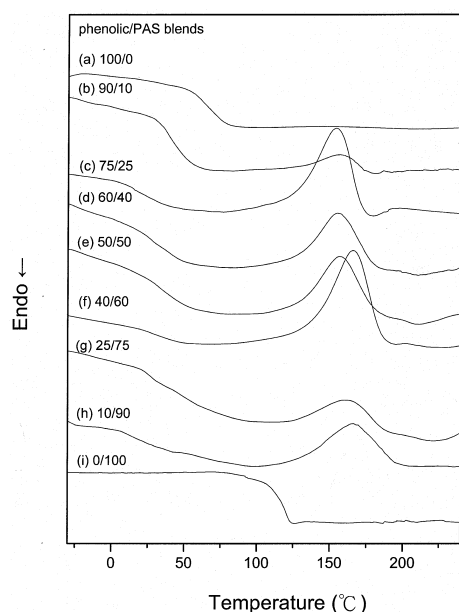
Figure 2. The DSC scans of phenolic/PAS blends with different compositions.
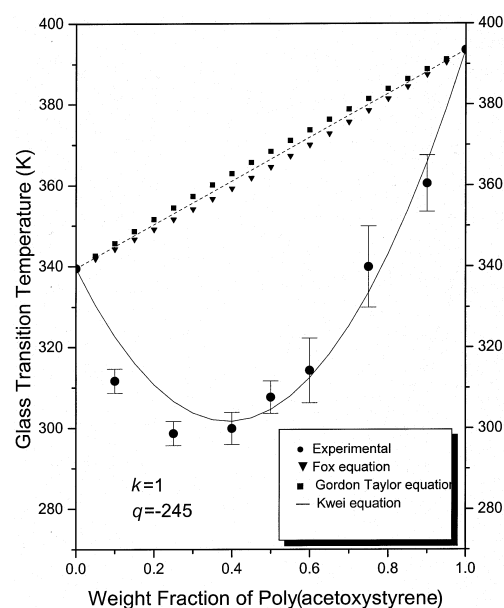
Figure 3. T_g versus composition curves from experimental data and the different fitting equations.

are obtained. Here q is a parameter corresponding to the strength of hydrogen bonding in the blend, reflecting a balance between the breaking of the self-association and the forming of the inter-association hydrogen bonding. The q value of the blend should depend on the entropy change corresponding to the change in the number of hydrogen bonding interactions. In this study, a negative q of "−245" was obtained, which indicates that the inter-molecular hydrogen bonding is weaker than the intra-molecular ones. The observed reduction in T_g levels in these phenolic/PAS blends is caused by the partial removal of the self-association of the intra-hydrogen bonding. Consequently, a special interaction must exist between these two base polymers to reduce the phenolic intra-molecular hydrogen bonding from DSC analyses.

FT-IR Analyses

Figure 4 displays the infrared spectra in the region 1 680 cm^{-1} to 1 820 cm^{-1} for various phenolic/PAS blend compositions measured at 25 °C. The carbonyl-stretching frequency is split into two bands at 1 760 cm^{-1} and 1 730 cm^{-1}, corresponding to the free and the hydrogen-bonded carbonyl groups, respectively. The hydrogen-bonded fraction of the carbonyl group increases with the phenolic content. The band can be easily decomposed into two Gaussian peaks, with areas corresponding to the hydrogen-bonded carbonyl (1 730 cm^{-1}) and free carbonyl (1 760 cm^{-1}). Provided the respective absorption coefficients are known, the relative fractions of free and hydrogen-bonded carbonyl groups can be calculated. The fraction of the hydrogen-bonded carbonyl groups[5] can be calculated from Equation (4):
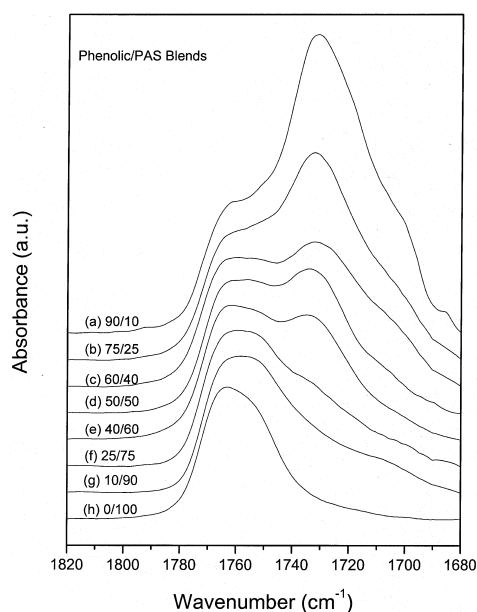
Figure 4. FT-IR spectra for different phenolic/PAS blends recorded at room temperature in the $1820\,\mathrm{cm^{-1}}$–$1680\,\mathrm{cm^{-1}}$ region.

Figure 5. FT-IR spectra for different phenolic/PAS blends recorded at room temperature in the $4000\,\mathrm{cm^{-1}}$–$2700\,\mathrm{cm^{-1}}$ region.

$$f_{\mathrm{b}}^{\mathrm{C=O}} = \frac{A_{\mathrm{b}}/1.5}{A_{\mathrm{b}}/1.5 + A_{\mathrm{f}}} \qquad (4)$$

where A_{b} denotes the peak area of the hydrogen-bonded carbonyl absorption and A_{f} represents the peak area of the free carbonyl absorption. The conversion coefficient 1.5 is the ratio of these two bands, free and hydrogen-bonded carbonyl groups, in an ester group.[5] Table 1 summarizes the results from curve fitting, indicating that the hydrogen-bonded fraction of the carbonyl group increases with the increase of the phenolic content.

The hydroxyl-stretching region of the phenolic/PAS blends is examined next. Figure 5 shows infrared spectra for the $2700\,\mathrm{cm^{-1}}$ to $4000\,\mathrm{cm^{-1}}$ regions of the pure phenolic polymer, pure PAS, and various phenolic/PAS blends. The pure phenolic polymer exhibits two bands in the hydroxyl-stretching region of the infrared spectrum. A very broad band centered at $3350\,\mathrm{cm^{-1}}$ is attributed to
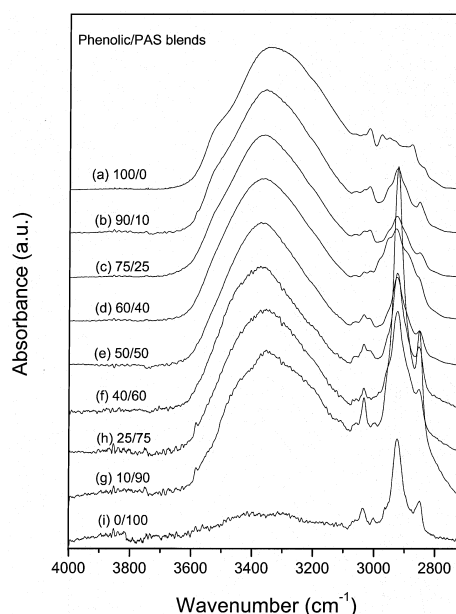
the wide distribution of the hydrogen-bonded hydroxyl group while a narrower shoulder band at $3525\,\mathrm{cm^{-1}}$ is caused by the free hydroxyl group.

Figure 5 also indicates that the intensity of free hydroxyl absorption ($3525\,\mathrm{cm^{-1}}$) decreases gradually as the PAS content of the blend is increased from 10 to 90 wt.-%. The band due to the hydrogen-bonded hydroxyl in the phenolic polymer tends to shift into a higher frequency with increasing PAS content in the vicinity of $3384\,\mathrm{cm^{-1}}$. This change results from the switch from the hydroxyl–hydroxyl bond to the hydroxyl–carbonyl bond. Therefore, it is reasonable to assign the band at 3384 $\mathrm{cm^{-1}}$ to the hydroxyl group that is bonded to the carbonyl group. The frequency difference between the free and the hydrogen-bonding hydroxyl has been used to investigate the average strength intermolecular interaction in our previous study.[19–22] In this study, the hydroxyl–carbonyl inter-association ($\Delta v = 139\,\mathrm{cm^{-1}}$) is weaker than that of

Table 1. Curve-fitting results of the phenolic/PAS blend at 25 °C.

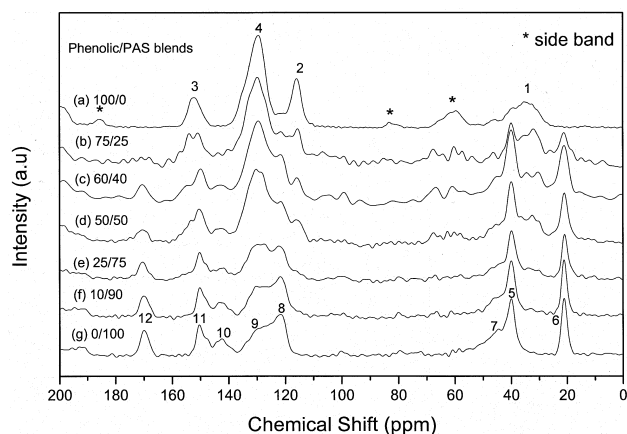| Phenolic/PAS wt.-%	free C=O			H-bonded C=O			f_{b}
	$\dfrac{v}{\mathrm{cm^{-1}}}$	$\dfrac{W_{1/2}}{\mathrm{cm^{-1}}}$	$\dfrac{A_{\mathrm{f}}}{\%}$	$\dfrac{v}{\mathrm{cm^{-1}}}$	$\dfrac{W_{1/2}}{\mathrm{cm^{-1}}}$	$\dfrac{A_{\mathrm{f}}}{\%}$	
90:10	1761.7	18.45	12.70	1731.2	37.50	87.30	82.10
75:25	1762.6	17.87	18.51	1732.1	39.13	81.49	74.59
60:40	1763.8	17.56	25.47	1732.4	38.49	74.53	66.12
50:50	1763.8	18.33	31.06	1736.8	39.70	68.94	59.68
40:60	1763.1	17.35	37.88	1738.2	38.92	62.12	52.23
25:75	1760.9	19.60	53.41	1735.9	39.63	46.59	36.77
10:90	1758.3	21.77	78.74	1728.6	43.87	21.26	15.26

Figure 6. ^{13}C CPMAS spectra at room temperature for different phenolic/PAS blends.

the self-associated hydroxyl of the phenolic polymer ($\Delta v = 175$ cm^{-1}) and this result is consistent with the negative q value according to the Kwei equation.

Solid-State NMR Analyses

The phenolic polymer is a proton donor possessing easily accessible hydroxyl groups while PAS is a proton acceptor containing one carbonyl group on each side chain. Solid-state NMR spectroscopy can provide a tool to clarify the phase behavior and morphology of polymer blends involving the hydrogen bond formation. Figure 6 displays the ^{13}C CP/MAS spectra of selected phenolic/PAS blends of various compositions, where the line (a) shows the peak assignments of four major peaks. The hydroxyl substituted carbon atom in the phenolic ring (C—OH) has a resonance peak at 152.1 ppm, while the peaks at 115.8 ppm and 129.4 ppm correspond to the *ortho*-unsubstitituted carbon atom and the other carbon atoms in the phenol ring, respectively. Meanwhile, the other resonance at 35 ppm corresponds to the methylene carbon atoms. The PAS spectrum is line (g) in Figure 6, showing eight resonance peaks; Figure 1 presents the corresponding carbon atoms.

The chemical shift of the carbonyl carbon atom of the PAS increases with the phenolic content (Figure 7). The variation in chemical shift can be interpreted as the extent of the intermolecular specific interaction between the components.[23–28] As illustrated in Figure 7, the carbonyl carbon atom of the PAS component shifts downfield as the phenolic content in the blend increases, implying the existence of intermolecular hydrogen-bonding interaction. The bond angle and interchain distance between the nearest neighbor are generally expected to change after a specific interaction is formed. Such a change creates a different chemical environment for the correlated carbon atom, thus changing the magnetic shielding and hence the chemical shift. The observed shift of the carbonyl carbon
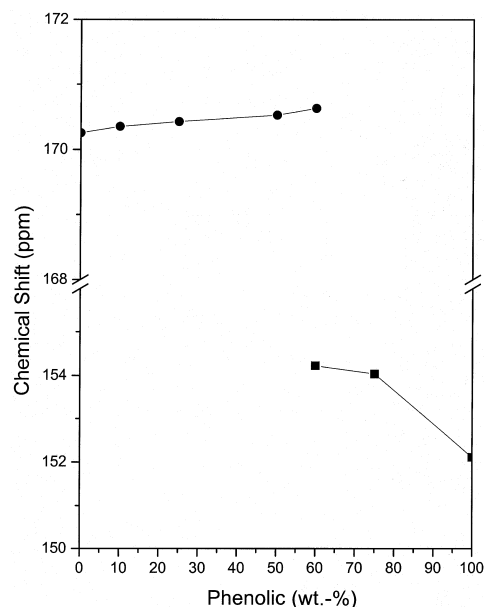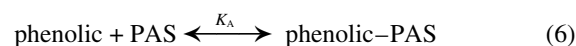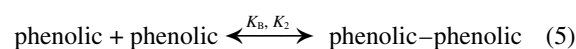

Figure 7. Composition dependence of the chemical shift of carbonyl group (●), the hydroxyl-substituted carbon (■) in the phenolic/PAS blends.

atom in this phenolic/PAS $= 60{:}40$ blend is 0.61 ppm higher than that of the pure PAS, a value which is comparable to other hydrogen-bonded miscible blends. Figure 7 also reveals a downfield shift of 2.1 ppm in the phenolic/PAS $= 60{:}40$ blend relative to the pure phenolic polymer, indicating strong intermolecular hydrogen bonding between the phenolic polymer and PAS.

Estimation of Inter-Association Equilibrium Constant (K_A)

According to the PCAM equation (Equation (2)), the $\Delta G_H/RT$ term is defined as the free-energy contribution owing to the change in hydrogen bonding upon mixing. A set of equilibrium constants, including self-association, inter-association, and other thermodynamic properties, must be determined to accurately predict the phase diagram, miscibility windows, and maps of polymer-blend systems involving specific interactions. The self-association of phenolic polymer involves the usual hydroxyl–hydroxyl interaction characteristics and requires two equilibrium constants, K_2 and K_B to account for the formation of the hydrogen-bonded dimer and multimer, respectively. The typical interaction scheme that was considered in the PCAM based on the competing equilibrium is described in Equation (5) and (6)

$$\text{phenolic} + \text{phenolic} \underset{}{\overset{K_B, K_2}{\rightleftharpoons}} \text{phenolic–phenolic} \quad (5)$$

$$\text{phenolic} + \text{PAS} \underset{}{\overset{K_A}{\rightleftharpoons}} \text{phenolic–PAS} \quad (6)$$

The inter-association equilibrium constant K_A reflects the extent of hydrogen bonding between phenolic poly-

mer and PAS. This study attempts to use PCAM to predict thermodynamic properties of this phenolic/PAS blend where the phenolic polymer contains a high density of hydroxyl groups.

To confirm the credibility of these association parameters of the phenolic polymer used in PCAM, the PAS has been chosen as an appropriate modifier to blend with the phenolic polymer. The p-tolyl acetate contains the carbonyl group that was selected as the model compound of PAS. The inter-association constant K_A of the PCAM describes the hydrogen-bonding interaction between the phenolic polymer and the PAS unit. The "free" hydroxyl bond absorptions of 0.02 M 2,4-dimethylphenol solution containing various concentrations of p-tolyl acetate in cyclohexane are used herein for quantitative measurements. Notably, the FT-IR from various concentrations of p-tolyl acetate solutions used as a background must be prescanned before addition of the 2,4-dimethylphenol. Figure 8 shows hydroxyl absorption of the 2,4-dimethylphenol in cyclohexane containing different concentrations of p-tolyl acetate, where the intensity of the free hydroxyl absorption at 3620 cm^{-1} decreases with increasing p-tolyl acetate concentration. The absolute intensity of the free hydroxyl group at 3620 cm^{-1} is assumed to be a measurement of the amount of free hydroxyl in the mixture. Figure 8 displays that the frequency of the associated hydroxyl band shifts from the free hydroxyl at 3620 cm^{-1} to 3510 cm^{-1} as the concentrations of p-tolyl acetate increases, because of the formation of inter-association hydrogen bonding between 2,4-dimethylphenol and p-tolyl acetate. The method proposed by Coggeshall and Saier,[29] involving the calculation of the hydrogen-bonding association constant, Ka (in L · mol^{-1}) is expressed by the following Equation (7):

$$Ka = \frac{1 - f_m^{OH}}{f_m^{OH}(C_A - (1 - f_m^{OH})(C_B)}$$ (7)

Where C_A and C_B denote the concentrations of p-tolyl acetate and 2,4-dimethylphenol in mol · L^{-1}, respectively, while f_m^{OH} represents the fraction of free hydroxyl of the 2,4-dimethylphenol. Table 2 lists the data on the level of f_m^{OH} for the 2,4-dimethylphenol containing various concentrations of p-tolyl acetate and the resulting Ka. The intrinsic inter-association constant Ka of $(10.67$ L · mol$^{-1})$ is obtained by extrapolating the p-tolyl acetate concentration of zero. Ka must be modified into K_A by dividing the molar volume of the phenolic repeated unit (0.083 L · mol^{-1} at 25 °C).[30] The inter-association equilibrium constant, K_A, yielded through this procedure is 128.60.

Figure 8 shows that the absorption frequency in the shift from the free hydroxyl (3620 cm^{-1}) to the hydrogen-bonding hydroxyl (3510 cm^{-1}) in the mixture of 2,4-dimethylphenol with p-tolyl acetate is concentration independent. The frequency difference between a free hydro-
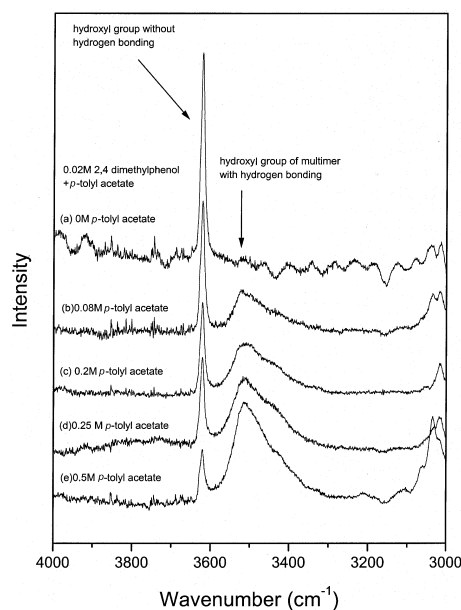

Figure 8. FT-IR spectra of the hydroxyl-stretching region of 0.02 M 2,4-dimethylphenol containing various p-tolyl acetate concentrations.

Table 2. f_m^{OH} and Ka of 2,4-dimethylphenol in cyclohexane solution with various p-tolyl acetate concentrations.

Conc. of p-tolyl acetate mol · L^{-1}	Intensity of IR Absorption	f^{OH}	Inter-association equilibrium constant (Ka^{model})
0	0.0321	1.0000	–
0.08	0.0185	0.5757	10.30203
0.1	0.0179	0.5571	8.7223
0.2	0.0128	0.3983	8.0341
0.25	0.0113	0.3517	7.7767
0.4	0.0097	0.3019	5.9900
0.5	0.0085	0.2645	5.7285

xyl and a hydrogen-bonding hydroxyl group can be roughly estimated from the enthalpy of the association and average strength in the polymer blend. In our previous study, we have proposed an equation to calculate the enthalpy of the association in the phenolic blend as given by the absorption shift, expressed here in Equation (8):[30]

$$-\Delta H = 2.564 + 0.0122\, \Delta v_{OH}\ (\text{cm}^{-1})$$ (8)

The enthalpy of the association between 2,4-dimethylphenol and p-tolyl acetate was calculated to be -3.88 Kcal · mol^{-1}. However, the K_A value obtained from model compounds is not exactly the same as that from the true polymer blend due to the intramolecular screening effect and functional group accessibility,[31–36] as well as the chain stiffness and connectivity in miscible polymer blends. Therefore, this investigation attempted to approximate another method proposed by Coleman et

al.[37] to obtain the K_A value, expressed by Equation (9) and (10)

$$\Phi_B = \Phi_{B1}\left[\left(1 - \frac{K_2}{K_B}\right) + \frac{K_2}{K_B}\left[\frac{1}{(1 - K_B\Phi_{B1})^2}\right]\right]$$

$$\left[1 + \frac{K_A\Phi_{0A}}{r}\right] \qquad (9)$$

$$\Phi_A = \Phi_{0A} + K_A\Phi_{0A}\Phi_{B1}\left[\left(1 - \frac{K_2}{K_B}\right) + \frac{K_2}{K_B}\right.$$

$$\left.\left[\frac{1}{(1 - K_B\Phi_{B1})}\right]\right] \qquad (10)$$

Where Φ_A and Φ_B are volume fractions of non-self-associated species A and self-associating species B, respectively, Φ_{0A} and Φ_{B1} are the corresponding volume fractions of isolated PAS and phenolic segment, respectively, and r is the ratio of molar volume, V_A/V_B. Self-association equilibrium constants, K_B and K_2, describe the formation of multimers and dimers, respectively. Finally, K_A is the equilibrium constant describing the association of A with B. In addition, K_B and K_2 of the phenolic polymer were set at 52.31 and 23.29, respectively, at 25 °C.[30] Employing these previously determined values of K_B and K_2 and a given value for K_A, together with the appropriate value of r, we can calculate and obtain the root (Φ_{B1}) numerical for a given value of Φ_B over the whole composition range. The fraction of hydrogen-bonded carbonyl groups as a function of the volume fraction of phenolic polymer is then simply given by $1-(\Phi_{0A}/\Phi_A)$. According to Table 1, the value of K_A is employed to determine the best fit of the experimental data for the phenolic/PAS blends at 25 °C using a least-squares method. Figure 9 displays the theoretical curves derived from the best-estimated value of $K_A = 64.6$.
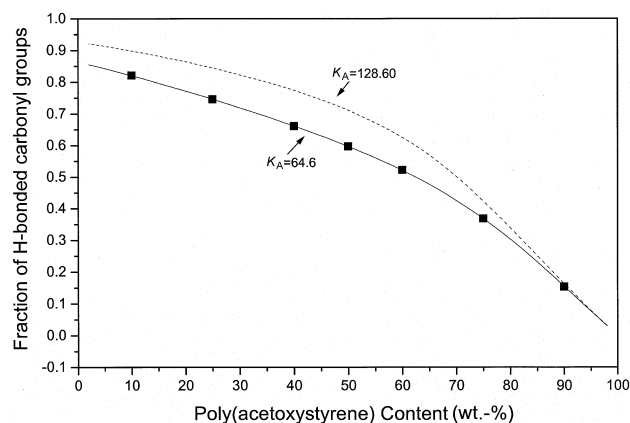

Figure 9. Fraction of the hydrogen-bonded carbonyl group versus composition: (■) FT-IR data, (- - -) theoretical values from model compounds and (—) theoretical values from polymer blend calculated at 25 °C.

The equilibrium constant, enthalpy of the phenolic/PAS blend, molar volume, molecular weight, and solubility parameters of the phenolic/PAS blend are summarized in Table 3. The observed $K_A = 128.6$ or 64.6 (model compound or polymer blend) is found to be much higher than the $K_2 = 23.29$ from the hydroxyl dimer formation and the $K_B = 52.31$ from the hydroxyl multimer formation, implying that the tendency of the phenolic resin to form the hydrogen bonding with PAS dominates over the self-association forming the intra-hydrogen bonding of the phenolic resin in the mixture.

Prediction of Degree of Hydrogen Bonding

Figure 9 shows plots of the experimental data and theoretical predicted curve as a function of composition at 25 °C, and demonstrates the ability of PCAM to predict the degree of hydrogen bonding on the carbonyl group. Figure 9 shows that the experimental values are generally

Table 3. Summary of the self-association and inter-association parameters of the phenolic/PAS blend.

	Equilibrium constant K 25°C	Enthalpy ΔH kcal·mol^{-1}
Self-association[a]		
Dimer formation K_2	23.29	−4.246
Multimer formation K_B	52.31	−6.110
Inter-association from model compound	128.60	−3.875
Inter-association from polymer blend	64.6	−3.875

Polymer	Molar volume mL·mol^{-1}	Molecular weight g·mol^{-1}	Solublity parameter (cal·mL^{-1})$^{0.5}$	Degree of polymerization
Phenolic[a]	84	105	12.05	6
PAS[b]	128.60	162.20	10.29	132

[a] Ref.[30]
[b] Estimated using a group contribution method proposed by Coleman et al.[5]

lower than the predicted values based on model compounds ($K_A = 128.6$) due to two of the more important chain connectivity effects, intramolecular screening and functional group accessibility. However, the experimental values show excellent agreement with the predicted values from the polymer blend ($K_A = 64.6$) for the hydrogen bonded carbonyl at 25 °C. Therefore, the inter-association constant $K_A = 64.4$ for the phenolic/PAS blend is considered to be valid. The inter-association equilibrium constant between polymer blend and model compound should therefore be different after taking into account the intramolecular screening and functional group accessibility effects.

Prediction of Free Energy

The calculation follows the 'Miscibility Guide and Phase Calculator' software package.[5] The path to correlate the hydrogen-bonding equilibrium concentration to the free-energy values has been described by Coleman et al.[5] Figure 10 illustrates that the predicted free energy (ΔG_m) is negative for all compositions at 125 °C. ΔG_m reached a minimum of -3.47 cal · cm^{-3} when the PAS content was around 66 wt.-%. The theoretically predicted values were compared with the experimental results at 125 °C because this temperature exceeds the T_gs of pure phenolic polymer and PAS, and because these DSC thermograms were obtained by quenching from this temperature. It is therefore reasonable to assume that equilibrium conditions can be attained at this temperature. Although the original Painter–Coleman association model has been modified in recent papers,[6,31–36] we can also roughly consider the phenolic/PAS blend as being miscible due to negative free energy and the positive second derivative of the weight fraction.
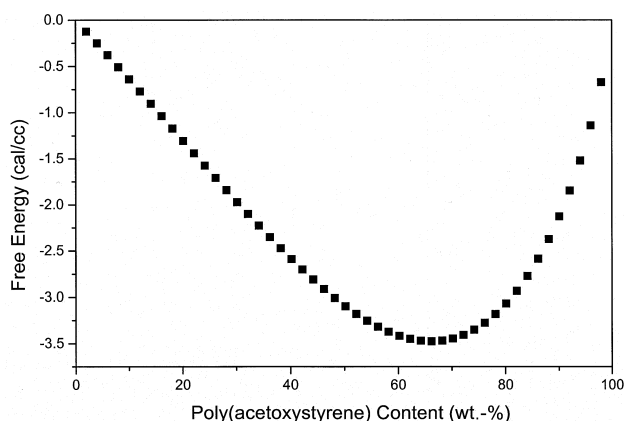

Figure 10. Calculated free energy of mixing against phenolic/PAS blend composition at 125 °C.

Phase Separation

Figure 2 presents DSC traces from all compositions heated above their T_gs. All blends show an exothermal
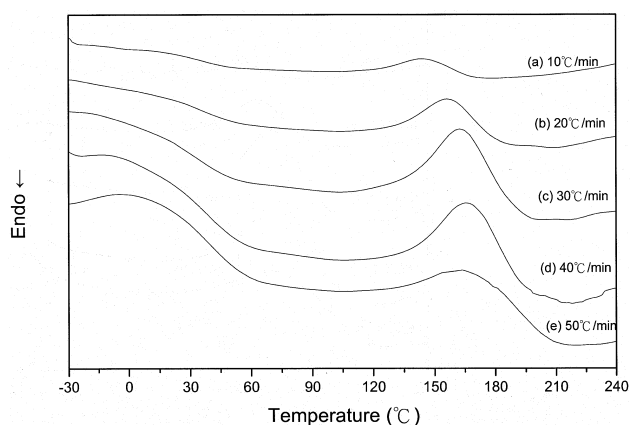

Figure 11. The DSC thermograms of the phenolic/PAS = 50:50 blend under different heating rates.
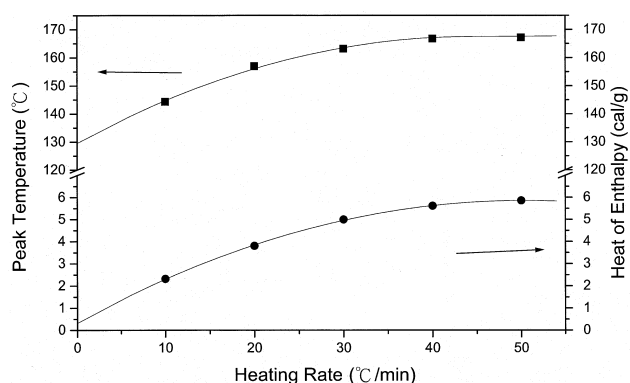

Figure 12. Exothermic peak temperature (■) and its heat enthalpy (●) of the phenolic/PAS = 50:50 versus different heating rates.

peak above their T_gs, which can be assigned to decomplexation or phase separation.[38–46] The exothermic peak temperature and its enthalpy depend on the DSC heating rate as shown in Figure 11 for the phenolic/PAS = 50:50 blend. Figure 12 displays the effects of heating rate on this exothermic peak temperature and its enthalpy, revealing that both increase with increased heating rate. Extrapolation of the demixing-peak temperature to zero heating rate (thermodynamic equilibrium condition) should produce the corresponding pseudobinodal or "cloud point" in the phase diagram[43] which is at 129.5 °C (Figure 12). On the other hand, the extrapolation to large heating rates is related to the spinodal temperature[43] which is at 169.5 °C (Figure 12).

Heat of Demixing

At high heating rates, the plateau value for the area of the exothermal peak can be considered to be the demixing heat for the blend, that is 5.88 cal · g^{-1}. In a nonequilibrium state, the blend is forced to transform from a single phase to a two-phase system, and the heat release becomes a measure of the two components' interaction.
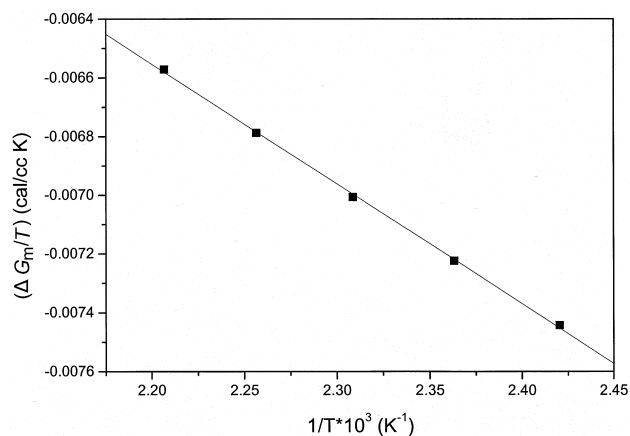
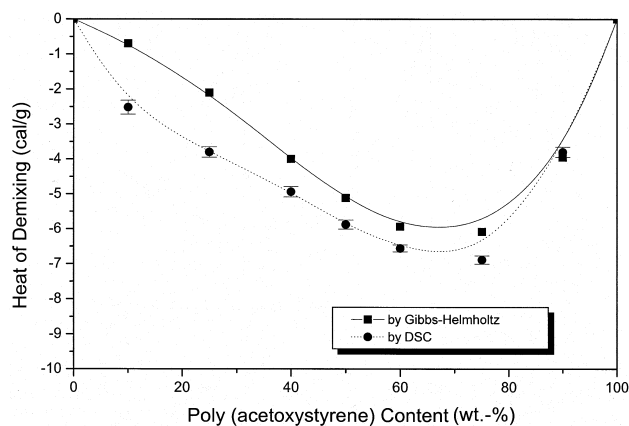Figure 13. $\Delta G_{\mathrm{m}}/T$ versus $1/T$ for the phenolic/PAS = 50:50 blend.

Figure 14. Heat of demixing versus blend composition for various phenolic/PAS blends derived from Gibbs–Helmholtz and DSC results.

Indeed, the plateau value of the peak area reflects the nature of the interaction of the components.

If the calculation is repeated at different temperatures for a single mixture (50:50) and the classic Gibbs–Helmholtz expression is employed by Equation (11):

$$\Delta H_{\mathrm{M}} = \partial(\Delta G_{\mathrm{M}}/T)/\partial(1/T) \qquad (11)$$

Then the enthalpy of mixing (ΔH_{M}) of a polymer pair can be calculated over a range of temperatures. Using the free energy of between 140 °C and 180 °C the mixing enthalpy can be calculated. Figure 13 plots $\Delta G_{\mathrm{m}}/T$ versus $1/T$ for the phenolic/PAS = 50:50 blend following the expression of Gibbs–Helmholtz. In the temperature range investigated herein, the relationship is linear, and the enthalpy of mixing of $-4.08 \ \mathrm{cal \cdot cm^{-3}}$ can be determined by its slope. A reasonable estimate of the specific volume for a 50:50 mixture of phenolic resin and PAS is $1.257 \ \mathrm{cm^3 \cdot g^{-1}}$ which gives an enthalpy of mixing of $-5.12 \ \mathrm{cal \cdot g^{-1}}$. This obtained enthalpy of mixing is close to the value experimentally obtained by DSC

($-5.88 \ \mathrm{cal \cdot g^{-1}}$) for the phenolic/PAS blend. Figure 14 shows the enthalpy of demixing against blend composition for phenolic/PAS blends based on results from the Gibbs–Helmholtz approach and from the phase separation in DSC. Figure 14 reveals that demixing of phenolic/PAS blends is exothermic and the trend of enthalpy of demixing determined by DSC is similar to the calculated from the Gibbs–Helmholtz approach based on PCAM. Apparently, the enthalpy of demixing measured by DSC can be accepted as the real enthalpy of demixing for blends. Also shown in Figure 14, the enthalpy of demixing from the Gibbs–Helmholtz approach and from DSC results in a minimum value at about 66 wt.-%, exhibiting the same trend as in Figure 10.

Evidence of Phase Separation via FT-IR Analyses

Figure 15 illustrates the FT-IR spectra of the phenolic/PAS = 50:50 blend measured at different temperatures in the range 25 °C to 180 °C. The carbonyl-stretching frequency splits into two bands at $1\,760 \ \mathrm{cm^{-1}}$ and $1\,730 \ \mathrm{cm^{-1}}$, corresponding to the free and hydrogen-bonded carbonyl groups, respectively. The intensity of the hydrogen-bonded carbonyl group decreases with increasing temperature. As a result, the quantity of the $\Delta G_{\mathrm{H}}/RT$ term of Equation (2) will decrease with increasing the temperature, and when the measured temperature reaches a critical level, this negative chemical term, $\Delta G_{\mathrm{H}}/RT$ will be unable to overcome the positive physical term, $\chi_{12}\Phi_1\Phi_2$ and results in positive free energy of mixing and phase separation, according to Equation (2). Figure 16 shows the corresponding fraction of free carbonyl groups versus temperature. The fraction of the free carbonyl
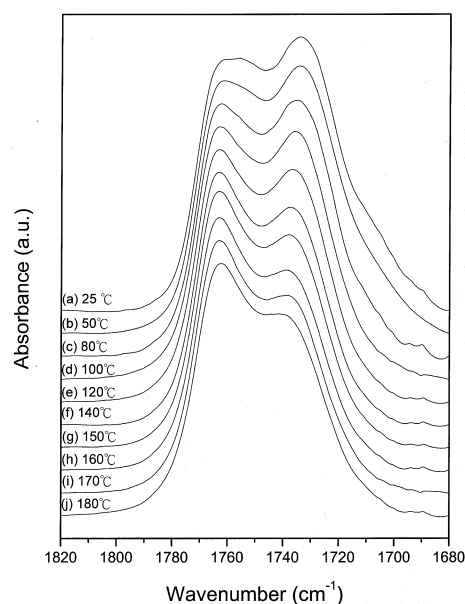

Figure 15. FT-IR spectra recorded at various temperatures at $1\,820 \ \mathrm{cm^{-1}}$–$1\,680 \ \mathrm{cm^{-1}}$ region for phenolic/PAS = 50:50 blend.
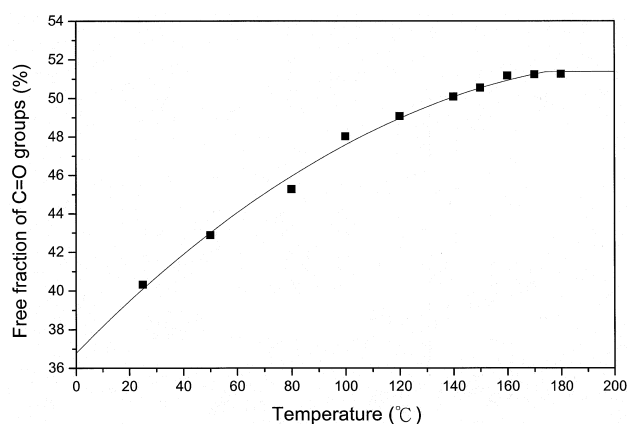
Figure 16. The fraction of free carbonyl groups versus temperature for the phenolic/PAS = 50:50 blend.

group approaches a plateau, an indication that the phase separation is approaching completion.

Conclusions

Phenolic resin and PAS are completely miscible over the entire composition range. The Kwei equation can accurately predict T_gs from the experimental results owing to the existence of hydrogen bonding between the hydroxyl group in the phenolic resin and the carbonyl group in PAS.

The inter-association equilibrium constant (K_A) for the phenolic/PAS blend is higher than the self-association equilibrium constants (K_2 and K_B), implying that the tendency toward hydrogen bonding of the phenolic resin and PAS dominates the self-association (intra-hydrogen bonding) of the phenolic resin in the mixture. However, the average strength of the inter-hydrogen bonding is weaker than that of the self-associated hydroxyl groups of the phenolic resin. The relatively weak interaction from the hydrogen bonding causes the observed T_g negative deviation compared with the Kwei equation.

The phase behavior of this miscible polymer blend has been analyzed by DSC and the enthalpy of demixing has been obtained, which agrees with the Gibbs–Helmholtz expression where the free energy is derived from the Painter–Coleman association model. Above the lower critical solution temperature, the phase separation occurs due to gradual decrease of the inter-hydrogen bonding at higher temperatures that can be characterized by FT-IR analyses.

[1] H. D. Wu, C. C. M. Ma, P. P. Chu, H. T. Tseng, C. T. Lee, *Polymer* **1998**, *39*, 2859.
[2] Z. Zhong, Q. Guo, *Polymer* **1998**, *39*, 517.
[3] X. Li, S. H. Goh, Y. H. Lai, A. T. S. Wee, *Polymer* **2000**, *41*, 6563.
[4] C. Sawateri, T. Kondo, *Macromolecules* **1999**, *32*, 1949.
[5] M. M. Coleman, J. F. Graf, P. C. Painter, *"Specific Interactions and the Miscibility of Polymer Blends"*, Technomic Publishing, Lancaster, PA 1991.
[6] M. M. Coleman, P. C. Painter, *Prog. Polym. Sci.* **1995**, *20*, 1.
[7] M. J. Fernandez, M. Valero, D. I. Martinez, J. J. Iruin, *Polymer* **1999**, *34*, 28.
[8] D. I. Martinez, J. J. Iruin, M. J. Fernandez, *Macromolecules* **1995**, *28*, 3707.
[9] L. C. Cesteros, E. Meaurio, I. Katime, *Macromolecules* **1993**, *26*, 2323.
[10] A. Prinos, A. Dompros, A. Panayiotou, *Polymer* **1998**, *39*, 3011.
[11] L. A. Kanis, F. C. Viel, J. S. Crespo, J. R. Bertolino, T. N. Pires, V. Soldi, *Polymer* **2000**, *41*, 3303.
[12] X. Yang, P. C. Painter, M. M. Coleman, *Macromolecules* **1992**, *25*, 4996.
[13] N. Mekhilef, P. Hadjiandreou, *Polymer* **1995**, *36*, 2165.
[14] H. D. Wu, P. P. Chu, C. C. M. Ma, F. C. Chang, *Macromolecules* **1999**, *32*, 3097.
[15] H. D. Wu, C. C. M. Ma, P. P. Chu, *Polymer* **1997**, *38*, 5419.
[16] T. J. Kwei, *J. Polym. Sci., Polym. Lett. Ed.* **1984**, *22*, 307.
[17] M. Gordon, J. S. Taylor, *J. Appl. Chem.* **1952**, *2*, 493.
[18] T. G. Fox, *J. Appl. Bull. Am. Phys. Soc.* **1956**, *1*, 123.
[19] S. W. Kuo, F. C. Chang, *Macromolecules* **2001**, *34*, 4089.
[20] S. W. Kuo, F. C. Chang, *Macromolecules* **2001**, *34*, 5224.
[21] S. W. Kuo, F. C. Chang, *Macromolecules* **2001**, *34*, 7737.
[22] S. W. Kuo, C. F. Huang, F. C. Chang, *J. Polym. Sci., Polym. Phys. Ed.* **2001**, *39*, 1348.
[23] J. Wang, M. K. Cheung, Y. Mi, *Polymer* **2001**, *42*, 2077.
[24] T. Miyoshi, K. Takagoshi, T. Terao, *Macromolecules* **1999**, *32*, 8914.
[25] X. Zhang, K. Takegoshi, K. Hikichi, *Macromolecules* **1992**, *25*, 2336.
[26] J. Straka, P. Schmidt, J. Dybal, B. Schneider, J. Spevacek, *Polymer* **1995**, *36*, 1147.
[27] T. Miyoshi, K. Takegoshi, K. Hikichi, *Polymer* **1996**, *37*, 11.
[28] D. J. T. Hill, A. K. Whittaker, K. W. Wong, *Macromolecules* **1999**, *32*, 5285.
[29] N. D. Coggesthall, E. L. Saier, *J. Am. Chem. Soc.* **1951**, *71*, 5414.
[30] C. C. M. Ma, H. D. Wu, P. C. Chu, T. T. Han, *Macromolecules* **1997**, *30*, 5443.
[31] P. C. Painter, B. Veytsman, S. Kumar, S. Shenoy, J. F. Graf, Y. Xu, M. M. Coleman, *Macromolecules* **1997**, *30*, 932.
[32] M. M. Coleman, G. J. Pehlert, P. C. Painter, *Macromolecules* **1996**, *29*, 6820.
[33] G. J. Pehlert, P. C. Painter, B. Veytsman, M. M. Coleman, *Macromolecules* **1997**, *30*, 3671.
[34] G. J. Pehlert, P. C. Painter, M. M. Coleman, *Macromolecules* **1998**, *31*, 8423.
[35] M. M. Coleman, K. S. Guigley, P. C. Painter, *Macromol. Chem. Phys.* **1999**, *200*, 1167.
[36] P. C. Painter, M. M. Coleman, *"Polymer Blends"* Vol. 1, D. R. Paul, Ed., John Wiley & Sons, New York 2000.
[37] M. M. Coleman, A. M. Lichkus, P. C. Painter, *Macromolecules* **1989**, *22*, 586.

[38] S. Shen, J. M. Torkelson, *Macromolecules* **1992**, *25*, 721.

[39] C. C. Luis, R. I. Jose, I. Katime, *Macromolecules* **1994**, *27*, 7887.

[40] X. Chen, Z. Sun, J. Yin, L. An, *Polymer* **2000**, *41*, 5669.

[41] G. Dreezen, G. Groeninckx, S. Swier, B. V. Mele, *Polymer* **2001**, *42*, 1449.

[42] X. Chen, L. An, L. Li, J. Yin, Z. Sun, *Macromolecules* **1999**, *32*, 5905.

[43] A. Natansohn, *J. Polym. Sci., Polym. Lett. Ed.* **1985**, *23*, 305.

[44] M. Ebert, R. W. Garbella, J. H. Wendorff, *Macromol. Rapid Commun.* **1986**, *70*, 65.

[45] P. G. Tait, *Phys. Chem.* **1989**, *2*, 1.

[46] C. Uriarte, J. I. Eguiazabal, M. Llanos, J. I. Iribarren, J. J. Iruin, *Macromolecules* **1987**, *20*, 3038.